

Megaesophagus Is a Major Pathological Condition in Rats With a Large Deletion in the *Rbm20* Gene

Veterinary Pathology
2020, Vol. 57(1) 151-159
© The Author(s) 2019
Article reuse guidelines:
sagepub.com/journals-permissions
DOI: 10.1177/0300985819854224
journals.sagepub.com/home/vet



Denise J. Schwahn¹ , Jonathan M. Pleitner² ,
and Marion L. Greaser²

Abstract

A spontaneously arising, loss-of-function mutation in the RNA binding motif protein 20 (*Rbm20*) gene, which encodes a nuclear splicing protein, was previously identified as the underlying reason for expression of an abnormally large TITIN (TTN) protein in a rat model of cardiomyopathy. An outbreak of *Pseudomonas aeruginosa* led to submission of rats with dyspnea, sneezing, lethargy, nasal discharge, and/or unexpected death for diagnostic evaluation. Necropsy revealed underlying megaesophagus in *Rbm20*^{-/-} rats. Further phenotyping of this rat strain and determination of the size of esophageal TTN was undertaken. The *Rbm20*-defective rats developed megaesophagus at an early age (26 weeks) with high frequency (13/32, 41%). They also often exhibited secondary rhinitis (9/32, 28%), aspiration pneumonia (8/32, 25%), and otitis media/interna (6/32, 19%). In addition, these rats had a high prevalence of hydronephrosis (13/32, 41%). RBM20 is involved in splicing multiple RNA transcripts, one of which is the muscle-specific protein TTN. *Rbm20* mutations are a significant cause of dilated cardiomyopathy in humans. In *Rbm20*-defective rats, TTN size was significantly increased in the skeletal muscle of the esophagus. Megaesophagus in this rat strain (maintained on a mixed genetic background) is hypothesized to result from altered TTN stretch signaling in esophageal skeletal muscle. This study describes a novel mechanism for the development of megaesophagus, which may be useful for understanding the pathogenesis of megaesophagus in humans and offers insights into potential myogenic causes of this condition. This is the first report of megaesophagus and other noncardiac pathogenic changes associated with mutation of *Rbm20* in any species.

Keywords

aspiration, cardiomyopathy, hydronephrosis, megaesophagus, otitis media, rat, rhinitis, striated muscle, titin

Megaesophagus is dilation of the esophagus. It can affect part of or the entire esophagus, may be congenital or acquired, and can reflect peripheral or central nervous system disease (afferent, interneuron, or efferent pathways), neuromuscular junction dysfunction, or muscular disease. In humans, megaesophagus is frequently due to lower esophageal sphincter achalasia (failure to relax), with subsequent retention of ingesta within the distal esophagus, inflammation of the wall (esophagitis), loss of ganglion cells, and dilation.^{7,42,44} Aspiration pneumonia is an important consequence of megaesophagus in several species and can cause significant mortality. Herein, we describe a hereditary rat model (designated the *Rbm20*^{-/-} rat) that recapitulates many features of megaesophagus, including aspiration pneumonia.

Megaesophagus has been described in humans, dogs, cats, horses, cattle, rats,^{1,6,17,41} mice,^{40,11} nonhuman primates,³² ferrets,² and camelids.⁴⁷ Its causes and morphological and functional changes in rats are briefly reviewed here. Idiopathic megaesophagus with mortality has been reported in rats.^{1,6,17,41} Aspiration pneumonia was identified in 1 report and esophageal impaction in another.^{17,41} In the case of esophageal

impaction, the rats were of the BHE nonobese diabetic strain, and the caudal half of the esophagus was dilated; there was local myodegeneration attributed to compression atrophy.⁴¹ One substrain of Long-Evans rats with a high prevalence of megaesophagus exhibited precardial esophageal dilation, decreased numbers of ganglion cells within the myenteric plexus of both the thoracic and abdominal portions of the esophagus, and decreased muscularis thickness in the thoracic portion.¹ This condition was considered hereditary and neurogenic.¹

¹Research Animal Resources Center and Muscle Biology Laboratory, University of Wisconsin, Madison, WI, USA

²Muscle Biology Laboratory, University of Wisconsin, Madison, WI, USA

Supplemental material for this article is available online.

Corresponding Author:

Denise J. Schwahn, Zoetis Research and Development, 333 Portage St, Kalamazoo, MI 49007, USA.

Email: denise.schwahn@gmail.com

Ninety percent of 3- to 4-month old rats carrying an additional copy of the *Poliovirus receptor-related 3* (*Pvr13*, *Nectin 3*, *CD113*) gene had megaesophagus with features of achalasia, and they exhibited myodegeneration, inflammation, and decreased numbers of myenteric ganglia.³⁷ The cause of achalasia may have been an effect of transgene insertion or a random mutation in a founder rat.³⁷ Surgical models of megaesophagus apply a constricting ring to the serosal aspect of the abdominal esophagus, causing distension of the middle third of the esophagus and thinning of the submucosa and muscularis.⁴² The muscularis reproducibly hypertrophies at the site of the ring-induced stenosis, and foci of aspiration pneumonia are common.⁴² Chemical models of megaesophagus use benzalkonium chloride, which denervates the esophagus, causing achalasia, megaesophagus, hypertrophy of the muscularis, and increased epithelial proliferation in rats.⁸

RNA binding motif protein 20 (RBM20) is an RNA-binding protein that regulates splicing of multiple cardiac proteins.¹⁶ Alternative splicing is an important control mechanism for sarcomeric protein function in the heart.^{16,48} Mutations in *RBM20* are a major cause of dilated cardiomyopathy in humans.^{16,27,31} Loss-of-function mutations in *RBM20* result in improperly spliced TTN, a protein that controls both sarcomeric length and passive myofiber stiffness, resulting in a longer sarcomere and subsequent cardiac dilation.^{16,49} Mutations in *RBM20* may also be a cause of statin-associated myopathy.³⁵ The hearts of mice with deletion of the RNA recognition motif of *Rbm20* exhibit decreased diastolic stiffness and increased cardiac fibrosis.³⁴ In addition, RBM20 is a splicing factor for Enigma homolog 1 (ENH1, PDLIM5, L9, ENH), a scaffolding protein found within striated myofibers, increasing the expression of a shorter splice isoform (ENH3).²⁰ Defects in *RBM20* are associated with an increased ratio of ENH1/ENH3, which promotes hypertrophy of cardiac myofibers and is hypothesized to be a mechanism of cardiomyopathy in humans.²⁰

The *Rbm20*-defective rat was discovered by chance during a developmental study on the giant protein TTN.¹³ Differently sized TTN isoforms are expressed from a single gene via alternative splicing in an age-dependent manner.^{13,27} In the developmental study, some rats expressed a much larger TTN than that of age-matched wild-type rats, and all rats with the larger TTN came from the same litter.¹³ The increased TTN size was due to an autosomal dominant 95-kb deletion in *Rbm20*, corresponding to the loss of exons 2 to 14 and disruption of its important role in alternative splicing.¹⁶ Over 30 different genes show altered splicing in this rat strain (herein designated *Rbm20*^{-/-}), but the changes in TTN appear to be the most significant.¹⁶ The *Rbm20*^{-/-} rat expresses a markedly enlarged TTN protein in striated myofibers of both cardiac and skeletal muscles.^{16,27,28} Adult *Rbm20*^{-/-} rats exhibit left ventricular dilation with increased diastolic parameters but no changes in systolic parameters or contractility.¹⁶ *Rbm20*^{-/-} rats have decreased exercise tolerance, electrocardiographic abnormalities, and a predisposition to arrhythmia and unexpected death, similar to humans with *RBM20* mutations.¹⁶ Histologically, in *Rbm20*^{-/-} rats, there is subendocardial fibrosis, and

ultrastructurally, there are abnormal myofibril arrangements, Z line streaming, and lipofuscin deposits.¹⁵ Elongated and flaccid TTN filaments are thought to lead to reduced myofibril recoil with a compensatory increase in collagen biosynthesis, leading to subendocardial fibrosis.¹⁶

The current study was undertaken to more completely characterize the phenotype of a spontaneously arising *Rbm20* mutation in rats linked to cardiac disease in humans and assess its suitability as a model of human megaesophagus. We identified a high incidence of megaesophagus with subsequent aspiration pneumonia, rhinitis, and/or otitis media with intralesional foreign material in *Rbm20*^{-/-} rats. Megaesophagus is hypothesized to be due to the abnormally large TTN isoform expressed in esophageal skeletal muscle, resulting in elongated sarcomeres, myofibers, and organ dilation. A high incidence of hydronephrosis was also noted.

Materials and Methods

Animals

Rbm20^{-/-} rats were maintained on a mixed genetic background consisting of 50% Brown Norway, 25% Fisher 344, and 25% Sprague-Dawley strains. Rats were cohoused in groups of 2 in open-topped cages in 2 separate conventional facilities with 12/12-hour light/dark cycles and stable temperature (22°F). Teklad standard rodent chow (Harlan, Madison, WI) and water were available ad libitum. Enrichment was provided to dams via a stainless steel loft. Animals housed singly were provided with a PVC tube and Nyla bones. Both colonies were free of rat coronavirus, rat theilovirus, *Pneumocystis carinii*, Sendai virus, pneumonia virus of mice, *Mycoplasma pulmonis*, rat reovirus 3, lymphocytic choriomeningitis virus, cilia-associated respiratory bacillus, Hantaan virus, *Clostridium piliforme*, mouse adenovirus 1, and mouse adenovirus 2. Positive serologic results were occasionally seen for a generic parvovirus antigen in both colonies. All rats were genotyped by polymerase chain reaction (PCR) as described previously.¹⁶ Animal care and use were in accordance with the Guide for Care and Use of Laboratory Animals published by the US National Institutes of Health (NIH publication 85-23, revised 1996), and all experimental procedures were approved by the University of Wisconsin Institutional Animal Care and Use Committee.

Case Inclusion Criteria

Thirty-two *Rbm20*^{-/-} rats of both sexes and ages 6 to 60 weeks, 4 *Rbm20*^{+/-} rats of both sexes and ages 10 to 47 weeks, and 6 *Rbm20*^{+/+} (wild-type) rats of both sexes and ages 6 to 84 weeks were included in this study. Initial cases in all 3 genotypes presented with clinical signs that included dyspnea, sneezing, nasal discharge, head tilt, buphthalmia, lethargy, and unexpected death (Suppl. Table S1). Clinically normal rats of all 3 genotypes were recruited for use as phenotypic comparisons. Rats of any genotype that had been experimentally manipulated in any way were excluded from this study.

Necropsy, Histology, and Photomicrography

All rats were euthanized via carbon dioxide inhalation. Immediately following sacrifice, rats of all genotypes were examined grossly by a board-certified veterinary pathologist (D.J.S.). Rats with clinical signs were subject to complete necropsy, including microbiological culture of relevant tissues. Rats lacking clinical signs were subject to an abbreviated necropsy procedure, which excluded detailed evaluation of the lower intestinal tract. External esophageal diameters were measured using a ruler on the widest portion of the unopened, flattened esophagus. Megaesophagus was defined as a maximal external esophageal diameter ≥ 5 mm. Subsequently, the entire esophagus and proximal (squamous) portion of the stomach were opened longitudinally and fixed as a Swiss roll, with the cervical esophagus in the center of the roll. In cases with clinical disease, fresh tissues (including brain, tongue, larynx, trachea, lungs, esophagus and proximal stomach, heart, thymus, entire emptied gastrointestinal tract, kidneys, adrenal glands, reproductive organs, bladder, spleen, preputial/clitoral glands) were placed into 10% neutral-buffered formalin or decalcification solution (head, left pelvic limb; Surgipath Decalcifier I, Leica Biosystems, Buffalo Grove, IL). In cases lacking clinical signs, fresh tissues (lungs, cardiopulmonary hilar lymph nodes, esophagus and cranial stomach, heart, thymus, and any grossly abnormal tissue) were placed into 10% neutral-buffered formalin or decalcification solution (head). After 24 hours of fixation, tissues were trimmed, processed, embedded in paraffin, sectioned at 5 μm , and stained with hematoxylin and eosin (HE) or Masson's trichrome for light microscopic evaluation. A board-certified veterinary pathologist (D.J.S.) examined tissues and graded esophageal thickness and fibrosis from rats of all genotypes. Esophageal wall thickness was measured using a stage micrometer. Fibrosis (blue staining of collagen in trichrome-stained sections) was graded on a 5-point scale where 0, 1, 2, 3, 4, and 5 were equivalent to none, minimal, mild, moderate, marked, and severe, respectively. Photomicrographs were taken with an Olympus DP26 camera (Olympus, Center Valley, PA) mounted on a Nikon Eclipse 50i microscope (Nikon, Melville, NY).

Agarose Gel Electrophoretic Fractionation of TTN Isoforms

The esophagi of both *Rbm20*^{+/+} ($n = 4-5$) and *Rbm20*^{-/-} ($n = 3$) rats were isolated and divided into 3 portions of approximately equal length; the portions were designated the cervical, cranial thoracic, and caudal thoracic segments based on anatomic location. The external esophageal diameter of all esophagi was < 5 mm; megaesophagus was not apparent in any rat. Muscle samples from each segment of each rat were collected and immediately flash-frozen in liquid nitrogen. Tissues were solubilized (1:50 w/v) in a sample buffer consisting of 8 M urea, 2 M thiourea, 3% sodium dodecyl sulfate w/v, 75 mM dithiothreitol, 0.03% bromophenol blue, and 0.05 M Tris-HCl, pH 6.8. Equal quantities were subjected to sodium dodecyl sulfate (SDS) gel

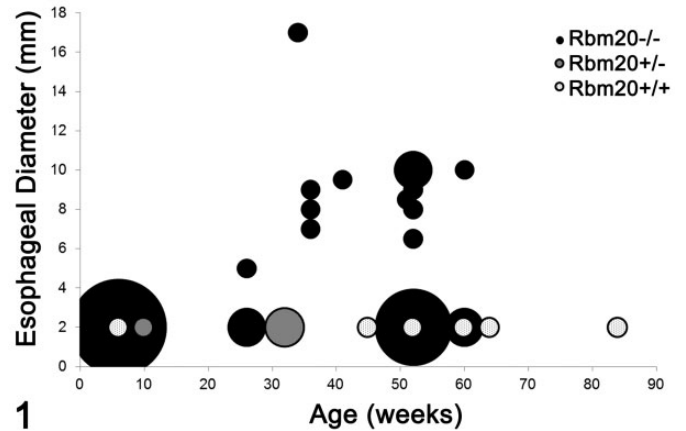


Figure 1. Bubble plot of closed esophageal diameter (mm) vs age (weeks) in rats of all *Rbm20* genotypes. The width of the bubble represents the number of rats with this age and esophageal diameter. Most animals of all genotypes and ages had esophageal diameters of 2 mm. Diameters larger than 5 mm were considered dilated; all rats with megaesophagus were *Rbm20*^{-/-}. Note that 1 heterozygote with megaesophagus did not have a measurement for the diameter; this animal is excluded from this plot.

electrophoresis in agarose.⁴⁶ Sizes were estimated using standards of *RBM20*^{-/-} cardiac TTN isoform (3.83 MDa) run in its own lane on the same gel and *RBM20*^{+/+} adult cardiac TTN N2B isoform (2.97 MDa), which was mixed with the esophageal protein samples. Molecular weights were estimated using the 2 standards and assuming a linear relationship between migration distance and the logarithm of the molecular mass.^{28,46}

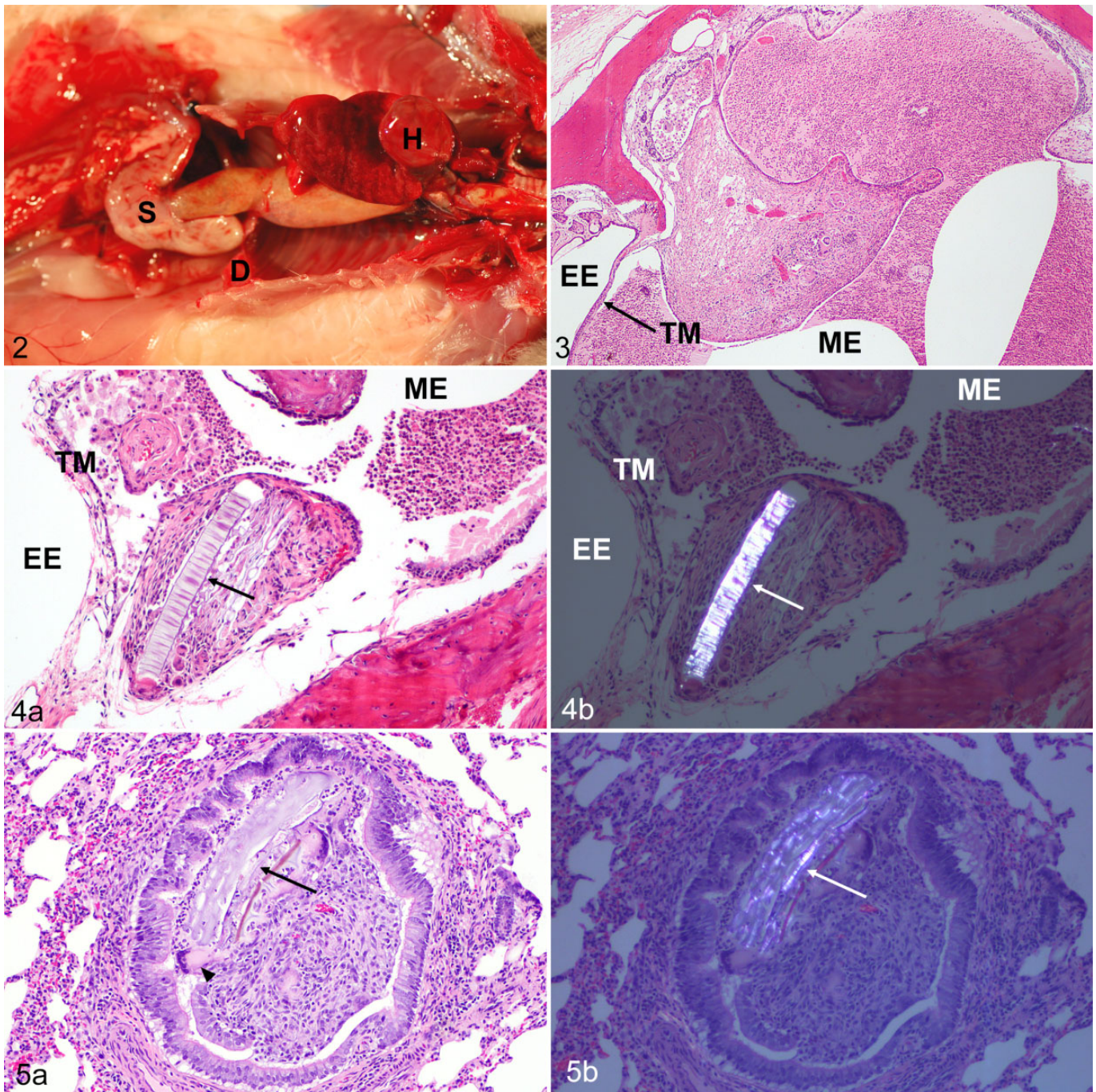
Statistical Analysis

Statistical analysis was performed using standard formulas within Microsoft Excel (Microsoft, Redmond, WA). *P* values were obtained using 2-tailed tests for equal variances.

The histologic slides and additional data analyzed in this study are available by request to the first author.

Results

For this study, 42 rats of all *Rbm20* genotypes (32 *Rbm20*^{-/-}, 4 *Rbm20*^{+/-}, and 6 wild-type) at 6 to 84 weeks of age were examined grossly and microscopically. Of the 32 *Rbm20*^{-/-} rats, 8 (25%) had clinical signs, including dyspnea, sneezing, lethargy, nasal discharge, and unexpected death; 24 had no clinical signs. One of the 4 (25%) *Rbm20*^{+/-} rats presented for sneezing; the others had no clinical signs. Four of the 6 (75%) wild-type rats presented with clinical signs that included sneezing, dyspnea, head tilt, buphthalmia, and unexpected death; the others lacked clinical disease. Megaesophagus was present in 13 of 32 (41%) *Rbm20*^{-/-} rats and 1 of 4 (25%) *Rbm20*^{+/-} rats (Fig. 1, Suppl. Table S1). In the 13 *Rbm20*^{-/-} rats with megaesophagus, the external esophageal diameters ranged from 5 to 17 mm; 8 females and 5 males were affected, and the youngest *Rbm20*^{-/-} animal with megaesophagus was 26 weeks old



Figures 2–5. Megaesophagus and aspiration pneumonia, 34-week-old *Rbm20*^{-/-} rat. The esophagus is markedly dilated; its closed esophageal diameter was 17 mm. D, remnant of removed diaphragm; H, heart; S, stomach. **Figures 3–4.** Chronic otitis media, 36-week-old *Rbm20*^{-/-} rat with megaesophagus. **Figure 3.** The middle ear (ME) cavity is filled by pyogranulomatous inflammation with thickening of the tympanic membrane (TM). Hematoxylin and eosin (HE). **Figure 4.** The middle ear contains viable and degenerate neutrophils admixed with macrophages, surrounding intralesional foreign material (a) that is birefringent under polarized light (b, arrow), indicating plant origin. HE. EE, external ear canal. **Figure 5.** Chronic aspiration pneumonia, 41-week-old *Rbm20*^{-/-} rat with megaesophagus. A bronchiole is filled with viable and degenerate neutrophils admixed with macrophages, some multinucleated (arrowhead), surrounding intralesional plant material (a) that refracts polarized light (b, arrow). HE.

(Fig. 1, Suppl. Table S1). Wild-type rats and rats without megaesophagus typically had esophageal diameters of 2 mm (Fig. 1, Suppl. Table S1). Megaesophagus always involved the intrathoracic and intra-abdominal portions of the esophagus

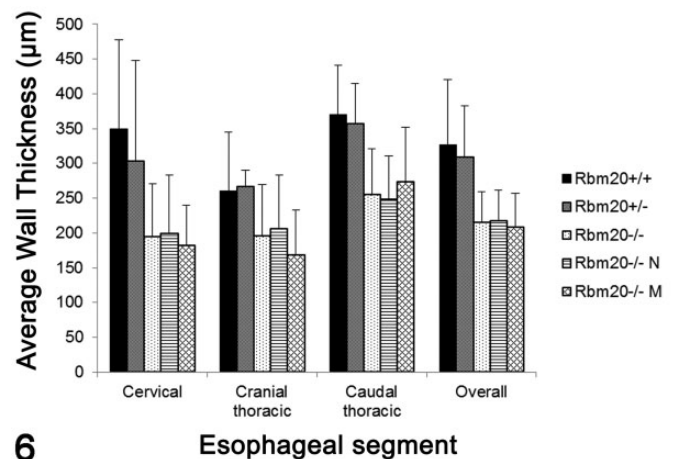
and never the cervical portion (Fig. 2). The esophageal diameter in the *Rbm20*^{+/-} rat with megaesophagus was not measured, but dilation was grossly apparent. This rat also presented with sneezing.

Of the 8 rats (5 *Rbm20*^{-/-}, 1 *Rbm20*^{+/-}, and 2 *Rbm20*^{+/+}) with clinical signs of upper respiratory disease (dyspnea, sneezing, and nasal discharge), all 8 had histologic evidence of aspiration pneumonia, rhinitis, and/or otitis media/interna (Figs. 3–5b, Suppl. Table S1). Three of the 5 rats (60%) that presented for lethargy or unexpected death also had histologic evidence of aspiration pneumonia, rhinitis, and/or otitis media/interna; all were *Rbm20*^{-/-}. Aspiration pneumonia, rhinitis, and/or otitis media/interna were identified histologically in an additional 3 rats (all *Rbm20*^{-/-}) that lacked clinical signs of respiratory disease, lethargy, or unexpected death and were apparently healthy (Suppl. Table S1).

A total of 12 *Rbm20*^{-/-} (11/32; 34%) or *Rbm20*^{+/-} (1/4; 25%) rats had histologic evidence of aspiration pneumonia, rhinitis, and/or otitis media/interna; of these rats, all also had megaesophagus. Megaesophagus was not identified in any *Rbm20*^{+/+} rat. Aspiration pneumonia, rhinitis, and otitis media/interna (with intralesional foreign plant material) are considered secondary to megaesophagus and represent reflux of esophageal contents. In the 14 rats with megaesophagus, the prevalence of rhinitis was 71%, the prevalence of aspiration pneumonia was 64%, and the prevalence of otitis media/interna was 43%. While gross evidence of megaesophagus was first seen at 26 weeks of age, the sequelae of aspiration pneumonia, rhinitis, and/or otitis media were not identified microscopically until 36 weeks of age. The most common pathogen isolated from cases of aspiration pneumonia, rhinitis, or otitis media/interna was *Pseudomonas aeruginosa*.

As megaesophagus is often associated with esophageal wall thinning, the average thickness of the esophageal wall was measured at 3 different locations (cervical, cranial thoracic, and caudal thoracic) on a Swiss roll section in rats of each genotype (Figs. 6–9). Substantial differences in the thickness of different segments of the esophagus were not apparent. The overall average esophageal wall thickness in *Rbm20*^{+/+} rats was 326.7 ± 94.3 μm ($P < .006$ vs *Rbm20*^{-/-}; $n = 6$ segments); esophageal walls were thinner in *Rbm20*^{+/-} rats (308.9 ± 74.0 μm, $P < .006$ vs *Rbm20*^{-/-}; $n = 9$ segments) and even thinner in *Rbm20*^{-/-} rats (215.2 ± 44.0 μm; $n = 54$ segments) (Fig. 6). Esophageal wall thickness was further subdivided by segment among *Rbm20*^{-/-} rats with and without grossly apparent megaesophagus, but no substantial difference was apparent (Fig. 6). Overall esophageal wall thickness was not significantly different between *Rbm20*^{-/-} rats with megaesophagus (208.0 ± 49.1 μm) and without megaesophagus (218.0 ± 43.7 μm; $P = .42$).

Fibrosis may be a component of esophageal wall thinning. To address this possibility, Masson's trichrome staining with numerical scoring of the amount of collagenous (blue) staining was used. Age-, sex-, and genotype-matched controls without megaesophagus were also examined (Figs. 7, 8). In 3 age- and sex-matched pairs of *Rbm20*^{-/-} rats with and without megaesophagus, the quantity of blue staining on trichrome-stained Swiss rolls of the esophagi was graded (data not shown). There was slightly less collagenous connective tissue staining in *Rbm20*^{-/-} animals with megaesophagus (Fig. 8b) than in



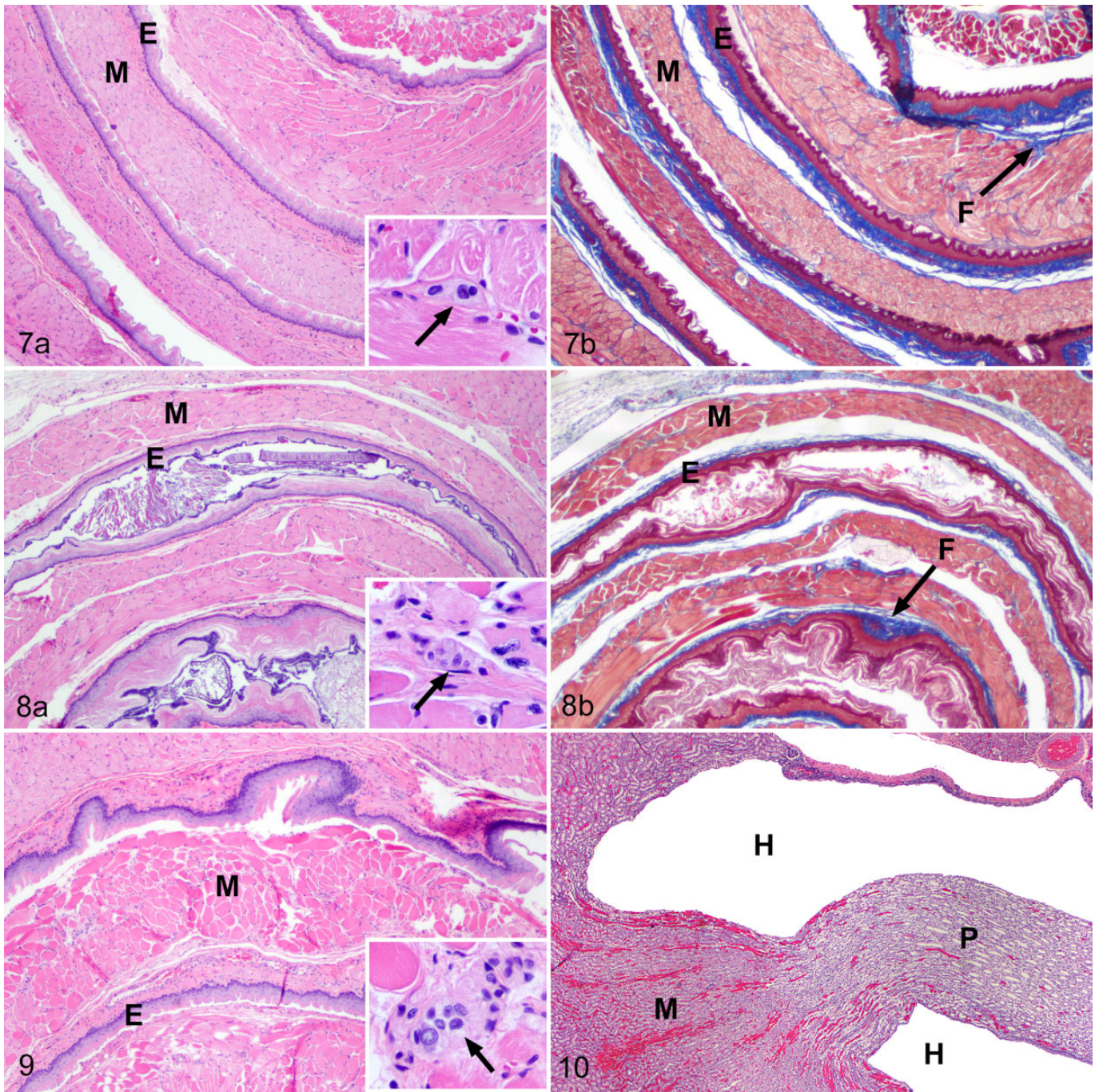
6 **Esophageal segment**

Figure 6. Average esophageal wall thickness shown by segment for rats of all *Rbm20* genotypes. “*Rbm20*^{-/-}” indicates all genotypically null animals, “*Rbm20*^{-/-} N” indicates genotypically null rats with esophagus of ≤5 mm, and “*Rbm20*^{-/-} M” indicates genotypically null rats with megaesophagus. The average thickness of the esophageal wall among all *Rbm20*^{-/-} rats was 194.4 ± 76.2 μm in the cervical portion, 195.6 ± 74.1 μm in the cranial thoracic portion, and 255.6 ± 65.3 μm in the caudal thoracic portion ($n = 18$). Standard deviations are depicted. $n = 2$ for *Rbm20*^{+/+} rats; $n = 3$ for *Rbm20*^{+/-} rats; $n = 13$ for *Rbm20*^{-/-} N rats, and $n = 5$ for *Rbm20*^{-/-} M rats.

Rbm20^{-/-} rats without megaesophagus (Fig. 7b), but the difference was not notable, and the histologic perception was of equal amount of collagen in the esophageal walls of both animals (Figs. 7, 8). The subjective decrease in fibrous tissue in rats with megaesophagus may be due to the same quantity of extracellular matrix and collagen spread over a greater area (due to dilation).

Megaesophagus may be due to decreased numbers or function of the submucosal or myenteric plexuses within the esophageal wall. Swiss roll sections of rat esophagi were examined for the presence of both plexuses as well as any histological abnormalities (Figs. 7–9). Submucosal plexuses were difficult to identify with HE or trichrome staining in any of the 47 rats examined, but myenteric plexuses were regularly encountered in rats of all *Rbm20* genotypes (Figs. 7a inset, 8a inset, 9 inset, and data not shown). Myenteric plexuses were counted in each animal, and the number of these plexuses did not differ by genotype (data not shown). No histologic abnormalities of the plexuses were noted. There were no differences in the number of ganglion cells within the submucosal and myenteric plexuses in animals with megaesophagus vs those with normal esophagi (data not shown). Inflammation was not identified in any portion of the esophagus in any rat.

An increased prevalence of hydronephrosis was also noted (Fig. 10, Suppl. Table S1). Either unilateral or bilateral hydronephrosis was identified in 14 rats (33%). Thirteen of these rats were *Rbm20*^{-/-} (7 females, 6 males), and one was *Rbm20*^{+/+} (female). The prevalence of hydronephrosis in *Rbm20*^{-/-} rats was 41% ($n = 32$), and the prevalence of hydronephrosis in



Figures 7–10. Esophageal Swiss rolls from rats of varying *Rbm20* genotypes. Figure 7 is from a 52-week-old *Rbm20*^{-/-} rat without megaesophagus, Figure 8 is from a 60-week-old *Rbm20*^{-/-} rat with megaesophagus, and Figure 9 is from a 64-week-old *Rbm20*^{+/+} rat without megaesophagus. In each case, all layers of the esophagus are present in appropriate ratios (a). Insets show normal ganglion cells (arrow) of the myenteric plexus. Similar amounts of fibrosis (F, blue) are seen in the submucosal regions in both the *Rbm20*^{-/-} rat lacking megaesophagus (Fig. 7b) and the *Rbm20*^{-/-} rat with megaesophagus (Fig. 8b); a similar amount of fibrosis was also seen in the *Rbm20*^{+/+} rat (data not shown). A, Hematoxylin and eosin (HE). B, Masson's trichrome. E, epithelium; M, muscularis. Figure 10. Hydronephrosis, 52-week-old *Rbm20*^{-/-} rat with megaesophagus. HE. H, dilated pelvis; M, medulla; P, papilla.

wild-type rats was 17% ($n = 6$). Hydronephrosis was not seen in *Rbm20*^{+/+} rats, possibly due to the small sample size ($n = 4$). Interestingly, 6 of the 13 (46%) *Rbm20*^{-/-} rats with hydronephrosis had concurrent megaesophagus, suggesting the possibility of a functional molecular link between the 2 conditions.

Seven of the 14 (50%) rats with hydronephrosis had associated urinary disease, such as urolithiasis (15%) or urinary tract infection (8%). The *Rbm20*^{+/+} rat with hydronephrosis died of septic pneumonia at 52 weeks of age and did not have evidence of concurrent urinary tract disease.

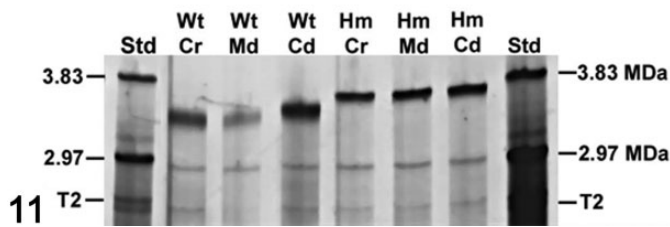


Figure 11. Agarose gel electrophoresis of TTN isoforms in different portions of the esophagus in *Rbm20*^{+/+} and *Rbm20*^{-/-} animals without megaesophagus. TTN isoforms are larger in all parts of the esophagus in *Rbm20*^{-/-} rats. All esophagus samples contain a band at 2.97 MDa (the predominant TTN isoform) from the deliberate addition of wild-type cardiac TTN for use as an internal size standard. Cd, caudal thoracic esophagus; Cr, cervical esophagus; Hm, *Rbm20*^{-/-}; Md, cranial thoracic esophagus; MDa, megadaltons; Std, mass standard; T2, a pro-teolytic fragment of TTN; Wt, *Rbm20*^{+/+}.

Given the role of RBM20 in splicing *Ttn* and TTN's role in determining the length of the sarcomere in striated myofibers, examination of the size of the TTN isoforms in *Rbm20*^{-/-} rats was undertaken. Large molecule gel electrophoresis of the 3 segments of the esophagi of *Rbm20*^{+/+} and *Rbm20*^{-/-} rats was used to determine the size of the TTN isoforms in the cervical, cranial thoracic, and caudal thoracic segments (Figs. 11,12). The TTN isoform seen in the *Rbm20*^{-/-} rats was much larger in all segments of the esophagi of *Rbm20*^{-/-} rats (~3700 kDa) compared with the isoform in *Rbm20*^{+/+} rats, which further appeared to vary by esophageal segment (~3460 kDa in the cervical portion, ~3490 kDa in the cranial thoracic portion, and ~3590 kDa in the caudal thoracic portion) (Fig. 12).

Discussion

This study was undertaken to further characterize the phenotype of *Rbm20*^{-/-} rats; a high prevalence of megaesophagus with secondary aspiration pneumonia, rhinitis, and/or otitis media was found. There was a close relationship between the presence of megaesophagus, aspiration pneumonia, rhinitis, otitis media, and clinical signs such as dyspnea, sneezing, and nasal discharge. Megaesophagus in *Rbm20*^{-/-} rats was first identified at 26 weeks of age, while the sequelae of aspiration pneumonia, rhinitis, and/or otitis media were first seen at 36 weeks of age. Megaesophagus in *Rbm20*^{-/-} and *Rbm20*^{+/-} rats is likely myogenic, as wall thinning was seen in rats of both genotypes regardless of the presence of megaesophagus. This finding supports the hypothesis that the *Rbm20* deletion mutation leads to aberrant *Ttn* splicing and more flaccid (thinner) myofibers and muscles. There was no evidence of increased esophageal wall fibrosis, histologic abnormalities of the ganglion cells of the submucosal or myenteric plexuses, or inflammation. The primary myogenic mechanism of megaesophagus in *Rbm20*^{-/-} rats is unique among rats with megaesophagus and also differs from most human cases, which tend to be neurogenic.⁷

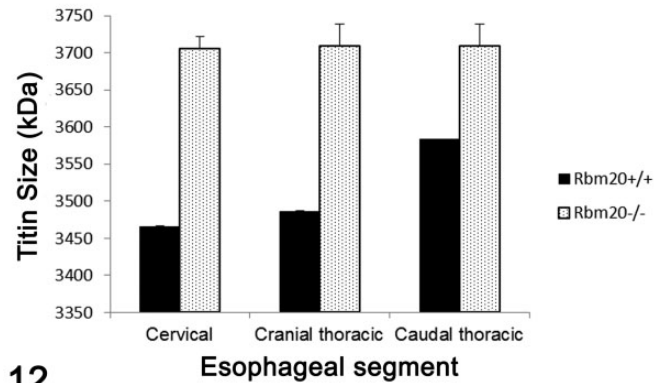


Figure 12. Larger TTN isoforms are seen in different portions of the esophagus in *Rbm20*^{-/-} rats without megaesophagus. The average TTN size in all parts of the esophagus of *Rbm20*^{-/-} rats was ~3700 kDa, while the average TTN size in wild-type rats was approximately 200 kDa less and varied from ~3460 kDa in the cervical portion to ~3590 kDa in the caudal thoracic portion. The data represent averages of multiple gels; standard deviations are depicted. *n* = 4 for *Rbm20*^{+/+} cervical segments; *n* = 5 for *Rbm20*^{+/+} cranial and caudal thoracic segments; *n* = 3 for *Rbm20*^{-/-} cervical, cranial thoracic, and caudal thoracic segments.

This study also found a similarly high prevalence of both megaesophagus (41%) and hydronephrosis (41%) in rats with a 95-kb, inactivating, autosomal dominant deletion of the *Rbm20* gene. The observed increased prevalence of hydronephrosis in *Rbm20*^{-/-} rats may be partly due to their genetic background. Congenital hydronephrosis is a common strain-related lesion in both Brown Norway and Sprague-Dawley rats, 2 of the 3 strains on which the *Rbm20* mutation is maintained, and a small contribution of these genetic backgrounds to the prevalence of hydronephrosis is expected.^{38,45} The prevalence of hydronephrosis was reported to be 67% to 75% in Brown Norway rats⁴³ and 2.0% to 5.1% in Sprague-Dawley rats.^{5,45} The *Rbm20*^{-/-} rats are 50% Brown Norway and 25% Sprague-Dawley, so the predicted prevalence of hydronephrosis in such a cross is approximately 34% to 40%. The observed prevalence of hydronephrosis in *Rbm20*^{+/+} rats was 17% (*n* = 6). The observed prevalence of hydronephrosis in *Rbm20*^{-/-} rats was 41%, which is slightly greater than expected, and almost half of *Rbm20*^{-/-} rats with megaesophagus also had hydronephrosis. Therefore, a link between loss of *Rbm20* function and hydronephrosis is possible. Interestingly, one of the transcripts spliced by RBM20 is *MECP2*, a gene whose duplication has been associated with hydronephrosis in human fetuses.⁹

RBM20 plays an important role in the development of megaesophagus in these rats, most likely through its action in splicing *Ttn*. The rat esophageal muscularis is composed entirely of striated myofibers.^{21,39,36} The TTN isoform seen in the esophagi of *Rbm20*^{-/-} rats is dramatically larger than the isoform in *Rbm20*^{+/+} rats; this is similar to what is seen in cardiac muscle and in several skeletal muscles of *Rbm20*^{-/-} rats.^{16,27,28,33} Identification of larger TTN isoforms in striated muscles of *Rbm20*^{-/-} rats strongly suggests that TTN is

improperly spliced in *Rbm20*^{-/-} rats. The larger TTN isoform lengthens individual sarcomeres,¹⁴ which is hypothesized to extend to longer myofilaments and myofibers with less passive tension, allowing the development of megaesophagus with secondary respiratory diseases such as aspiration pneumonia, rhinitis, and otitis media/interna. The failure to observe cervical esophageal dilation is attributed to differences in external esophageal pressures, where the cervical portion has high external pressure, and the thoracic and abdominal portions have low external pressures.

TTN extends the full length of the sarcomere and is physically linked to both the Z and M lines, thereby controlling sarcomere length. Larger TTN isoforms have additional amino acids from the inclusion of alternately spliced exons; the additional amino acids are found in the I band region, giving the myofibers (and muscle) a lower passive tension. TTN has also been suggested to act as a stretch sensor in cardiac and skeletal muscle.^{10,12,18,19,24,25,29,30} One signaling pathway involves a complex of TTN, muscle LIM protein (MLP), and telethonin (also called TCAP), through which MLP is translocated to the nucleus in response to stretch.^{22,23} Mutations in any of these 3 genes are associated with both dilated and hypertrophic cardiomyopathies in humans.³ In addition, the larger TTN isoforms expressed in the *Rbm20*^{-/-} rats and in humans lead to dilated cardiomyopathy in both species.^{4,16,26} Both decreased passive tension of myofibers containing enlarged TTN isoforms and reduced mechanical signaling by TTN are hypothesized to play roles in the pathogenesis of both cardiac and esophageal dilation in the *Rbm20*^{-/-} rat.^{16,26} The findings of this study suggest that expression of a very large TTN isoform (due to a large deletion in the *Rbm20* gene leading to failure of proper *Ttn* splicing) causes megaesophagus, with subsequent aspiration pneumonia, rhinitis, and otitis media/interna in rats. There is primary thinning of the esophageal muscularis. Fibrosis, inflammation, or neurogenic atrophy is not a driver of megaesophagus in *Rbm20*^{-/-} rats. The *Rbm20*^{-/-} rat exhibits a primary myogenic megaesophagus and may be a suitable model for myogenic cases of megaesophagus in humans, although most human cases are neurogenic. This is the first report of noncardiac pathogenic changes associated with an *Rbm20* mutation.

Acknowledgements

We thank Drs. Ruth Sullivan, Annette Gendron-Fitzpatrick, and Cynthia Bell for performing some of the diagnostic necropsies. Dr. Matt Rasette provided helpful discussions and clinical input early in the study. Ms. Beth Gray and Ms. Kelene Renberg provided expert technical assistance.

Declaration of Conflicting Interests

The author(s) declared no potential conflicts of interest with respect to the research, authorship, and/or publication of this article.

Funding

The author(s) received the following financial support for the research, authorship, and/or publication of this article: This work was

supported by the College of Agricultural and Life Sciences and grants from the National Institutes of Health (NIH) (HL77196 to M.L.G.) and the National Institute of Food and Agriculture, US Department of Agriculture (ID number WIS01556 to M.L.G.).

ORCID iD

Denise J. Schwahn  <https://orcid.org/0000-0001-8665-2402>

Jonathan M. Pleitner  <https://orcid.org/0000-0002-5236-2906>

References

- Baiocco A, Boujon CE, Hafeli W, et al. Megaesophagus in rats: a clinical, pathological, and morphometrical study. *J Comp Pathol*. 1993;**108**(3):269–281.
- Blanco MC, Fox JG, Rosenthal K, et al. Megaesophagus in nine ferrets. *J Am Vet Med Assoc*. 1994;**205**(3):444–447.
- Bos JM, Poley RN, Ny M, et al. Genotype-phenotype relationships involving hypertrophic cardiomyopathy-associated mutations in titin, muscle LIM protein, and telethonin. *Mol Genet Metab*. 2006;**88**(1):78–85.
- Brauch KM, Karst ML, Herron KJ, et al. Mutations in ribonucleic acid binding protein gene cause familial dilated cardiomyopathy. *J Am Coll Cardiol*. 2009;**54**(10):930–941.
- Chandra M, Frith CH. Non-neoplastic renal lesions in Sprague-Dawley and Fischer-344 rats. *Exp Toxicol Pathol*. 1994;**45**(7):439–447.
- Deerberg F, Pitterman W. Megaesophagus as the cause of death in rats. *Z Versuchstierkd*. 1972;**14**(4):177–182.
- Diamant N, Szczepanski M, Mui H. Manometric characteristics of idiopathic megaesophagus in the dog: an unsuitable animal model for achalasia in man. *Gastroenterology*. 1973;**65**(2):216–223.
- Febronio LH, Britto-Garcia D, de Oliveira JS, et al. Megaesophagus in rats. *Res Exp Med (Berl)*. 1997;**197**(2):109–115.
- Fu F, Liu HL, Li R, et al. Prenatal diagnosis of fetuses with congenital abnormalities and duplication of the MECP2 region. *Gene*. 2014;**546**(2):222–225.
- Gautel M. The sarcomeric cytoskeleton: who picks up the strain? *Curr Opin Cell Biol*. 2011;**23**(1):39–46.
- Ghaisas S, Srananth D, Deo MG. ICRC mouse with congenital mega-esophagus as a model to study esophageal tumorigenesis. *Carcinogenesis*. 1989;**10**(10):1847–1854.
- Granzier HL, Hutchinson KR, Tonino P, et al. Deleting titin's I-band/A-band junction reveals critical roles for titin in biomechanical sensing and cardiac function. *Proc Natl Acad Sci USA*. 2014;**111**(40):14589–14594.
- Greaser ML, Krzesinski PR, Warren CM. Developmental changes in rat cardiac titin/connectin: transitions in normal animals and in mutants with a delayed pattern of isoform transition. *J Mus Res Cell Motil*. 2005;**26**(6–8):325–332.
- Greaser ML, Warren CM, Esbona K, et al. Mutation that dramatically alters rat titin isoform expression and cardiomyocyte passive tension. *J Mol Cell Cardiol*. 2008;**44**(6):983–991.
- Guo W, Pleitner JM, Saupé KW. Pathophysiological defects and transcriptional profiling in the *Rbm20*(^{-/-}) rat model. *PLoS One*. 2013;**8**(12):e84281.
- Guo W, Schafer S, Greaser ML, et al. *Rbm20*, a gene for hereditary cardiomyopathy, regulates titin splicing. *Nat Med*. 2012;**18**(5):766–773.
- Harkness JE, Ferguson FG. Idiopathic megaesophagus in a rat (*Rattus norvegicus*). *Lab Anim Sci*. 1979;**29**(4):495–498.
- Hu X, Margadant FM, Yao M, et al. Molecular stretching modulates mechanosensing pathways. *Protein Sci*. 2017;**26**(7):1337–1351.
- Iskratsch T, Wolfenson H, Sheetz MP. Appreciating force and shape—the rise of mechanotransduction in cell biology. *Nat Rev Mol Cell Biol*. 2014;**15**(12):825–833.
- Ito J, Iijima M, Yoshimoto N, et al. *Rbm20* and *RBM24* cooperatively promote the expression of short enhancer splice variants. *FEBS Lett*. 2016;**590**(14):2262–2274.
- Kaufmann P, Lierse W, Stark J, et al. Muscle arrangement in the esophagus (man, rhesus monkey, rabbit, mouse, rat, seal). *Ergeb Anat Entwicklungsgesch*. 1968;**40**(3):3–33.

22. Knoll R, Buyandelger B. Z-disc transcriptional coupling, sarcomeroptosis and mechanopoptosis. *Cell Biochem Biophys*. 2013;**66**(1):65–71.
23. Knoll R, Hoshijima M, Hoffman H, et al. The cardiac mechanical stretch sensor machinery involves a Z disc complex that is defective in a subset of human dilated cardiomyopathy. *Cell*. 2002;**111**(7):943–955.
24. Krüger M, Kötter S. Titin, a central mediator for hypertrophic signaling, exercise-induced mechanosignaling and skeletal muscle remodeling. *Frontiers Physiol*. 2016;**7**:76.
25. Lange S, Xiang F, Yakovenko A, et al. The kinase domain of titin controls muscle gene expression and protein turnover. *Science*. 2005;**308**(5728):1599–1603.
26. Li D, Morales A, Gonzalez-Quintana J, et al. Identification of novel mutations in Rbm20 in patients with dilated cardiomyopathy. *Clin Transl Sci*. 2010;**3**(3):90–97.
27. Li S, Guo W, Dewey CN, et al. Rbm20 regulates titin alternation splicing as a splicing repressor. *Nucleic Acids Res*. 2013;**41**(4):2659–2672.
28. Li S, Guo W, Schmitt BM, et al. Comprehensive analysis of titin protein isoform and alternative splicing in normal and mutant rats. *J Cell Biochem*. 2012;**113**(4):1265–1273.
29. Linke WA. Sense and stretchability: the role of titin and titin-associated proteins in myocardial stress-sensing and mechanical dysfunction. *Cardiovasc Res*. 2008;**77**(4):637–648.
30. Linke WA, Krüger M. The giant protein titin as an integrator of myocyte signaling pathways. *Physiology (Bethesda)*. 2010;**25**(3):186–198.
31. Ma J, Lu L, Guo W, et al. Emerging role for RBM20 and its splicing substrates in cardiac function and heart failure. *Curr Pharm Des*. 2016;**22**(31):4744–4751.
32. Marsden PD, Seah SK, Draper CC, et al. Experimental *Trypanosoma cruzi* infections in rhesus monkeys. II. The early chronic phase. *Trans R Soc Trop Med Hyg*. 1976;**70**(3):247–251.
33. Mateja RD, Greaser ML, de Tombe PP. Impact of titin isoform on length dependent activation and cross-bridge cycling kinetics in rat skeletal muscle. *Biochim et Biophys Acta*. 2013;**1833**(4):804–811.
34. Methawasin M, Hutchinson KR, Lee EJ, et al. Experimentally increasing titin compliance in a novel mouse model attenuates the Frank-Starling mechanism but has a beneficial effect on diastole. *Circulation*. 2014;**129**(19):1924–1936.
35. Neroldova M, Stranecky V, Hodanova K, et al. Rare variant in known and novel candidate genes predisposing to statin-associated myopathy. *Pharmacogenomics*. 2016;**17**:1405–1414.
36. Nolte T, Brander-Weber P, Dangler C, et al. Nonproliferative and proliferative lesions of the gastrointestinal tract, pancreas, and salivary glands of the rat and mouse. *J Toxicol Pathol*. 2016;**29**(suppl 1):1S–124S.
37. Pang J, Borjeson TM, Muthupalani S, et al. Megaesophagus in a line of transgenic rats: a model of achalasia. *Vet Pathol*. 2014;**51**(6):1187–1200.
38. Proovost AP, van Aken M, Molenaar JC. Long-term follow-up of renal function in rats with unilateral hydronephrosis. *Scand J Urol Nephrol*. 1990;**24**(2):127–132.
39. Randelia HP, Deo MG, Lalitha VS. Megaesophagus in mouse: histochemical studies. *Gastroenterology*. 1988;**94**(5, pt 1):1243–1244.
40. Randelia HP, Lalitha VS. Megaesophagus in ICRC mice. *Lab Anim*. 1988;**22**(1):23–26.
41. Ruben Z, Rorhbacher E, Miller JE. Esophageal impaction in BHE rats. *Lab Anim Sci*. 1983;**33**(1):63–65.
42. Sons HU, Borchard F, Muller-Jah KL. Megaesophagus: induction by a simple animal experiment. *Exp Pathol*. 1986;**30**(4):193–201.
43. Spangler EL, Waggle KS, Hengemihle J, et al. Behavioral assessment of aging in male Fischer 344 and Brown Norway rat strains and their F1 hybrid. *Neurobiol Aging*. 1994;**15**(3):319–328.
44. van der Weyden L, Happerfield L, Arends MJ, et al. Megaesophagus in rassfla-null mice. *Int J Exp Path*. 2009;**90**(2):101–108.
45. Van Winkle TJ, Womack JE, Barbo WD, et al. Incidence of hydronephrosis among several production colonies of outbred Sprague-Dawley rats. *Lab Anim Sci*. 1988;**38**(4):402–406.
46. Warren CM, Krzesinski PR, Greaser ML. Vertical agarose gel electrophoresis and electroblotting of high molecular weight proteins. *Electrophoresis*. 2003;**24**(11):1695–1702.
47. Watrous BJ, Pearson EG, Smith BB, et al. Megaesophagus in 15 llamas: a retrospective study (1985–1993). *J Vet Intern Med*. 1995;**9**(2):92–99.
48. Weeland CJ, van den Hoogenhof MM, Beqqali A, et al. Insights into alternative splicing of sarcomeric genes in the heart. *J Mol Cell Cardiol*. 2015;**81**:107–113.
49. Wyles SP, Li X, Hrstka SC, et al. Modeling structural and functional deficiencies of Rbm20 familial dilated cardiomyopathy using human induced pluripotent stem cells. *Hum Mol Genet*. 2016;**25**(2):254–265.